2014 IEEE International Conference on Robotics & Automation (ICRA)
Hong Kong Convention and Exhibition Center
May 31 - June 7, 2014. Hong Kong, China

A hand/arm controller that simultaneously regulates internal grasp forces and the impedance of contacts with the environment

G. Muscio[†], F. Pierri[†], J. Trinkle[‡]

Abstract— **This paper presents a control framework for arm/hand systems aimed at controlling internal forces exchanged between the fingers and the grasped object, and enforcing a compliant behavior in presence of environmental interactions. A dynamic planner computes the motion references for the fingers by using the feedback of the contact forces, while an impedance control, in which dynamic effects exerted by the hand on the wrist are explicitly taken into account, is designed for the arm. The approach is experimentally validated on a 7-DOFs Barrett WAM with a Barrett Hand280.**

I. Introduction

Robotic applications relying on multi-fingered hands are challenging scenarios involving several fields, such as biomedical, service and prosthetic robotics. A key issue in robotic grasping is how to deal with the control of the contact forces applied by the fingertips to the grasped object, in such a way to prevent slippage and/or excessive stresses. At the same time, since robotic hands are often involved in strict contact with humans, a strategy to handle contacts with the external environment must be developed as well.

There are many works dealing with the problem of object manipulation and grasping. Useful surveys focused on contact modeling, multi-fingered robotics hands design and grasp properties can be found in [1], [2].

In order to cope with external environment interactions, the impedance control law is one of the most adopted strategies for robot manipulators [3]. Impedance concept has been successfully extended to multi-arm cooperative systems: in detail, in [4] the impedance paradigm is exploited to regulate internal contact forces and rigidly move the grasped object, while in [5] an impedance scheme is designed to confer a compliant behavior to the object (external impedance) and avoid large internal stresses to the object (internal impedance). For arm-hand systems impedance control approaches have been devised in [6], [7], where the virtual object concept is exploited to design an Intrinsically Passive Control (IPC) that can be used both for approaching the object and for grasping tasks. Others impedance control schemes for robotic hands have been proposed in [8], combined with an algorithm for grasp forces optimization, in [9], combined with an extended Kalman filter for friction estimation and in [10], where an impedance framework with multi-priority tasking is designed.

[†]School of Engineering of the University of Basilicata, via dell'Ateneo Lucano 10, 85100, Potenza, Italy {giuseppe.muscio, francesco.pierri}@unibas.it

[‡] Department of Computer Science Rensselaer Polytechnic Institute Troy, NY, 12180 USA.

An alternative to the impedance control is the adoption of hybrid force/position control schemes, as in [11], where the force on the fingers are seen as the sum of two orthogonal components: the manipulation force, necessary to impose object motion, and the grasping force, necessary to fulfill friction cone constraints. In [12] an hybrid impedance control is proposed for a robotic hand in order to recreate the movement and force of a human massage therapist: the lateral position of the robot fingertip is controlled by position-based impedance control, while the fingertip force for the vertical direction of human skin is controlled by force-based impedance control. Finally, parallel force/position control [13] can be adopted to reach both the reference position in the unconstrained directions and the reference forces in the constrained ones [14], [15], [16].

In this paper, a control framework for arm/hand systems is devised, which integrates an internal force control for the grasped object and an impedance control for the arm wrist, ensuring both a compliant behavior in the presence of environment interactions and that the object is held by the hand. More in detail, a dynamic planner, including the feedback of the measured contact forces, computes the motion references in Cartesian space for the fingers, that are fed to a standard inverse kinematics algorithm in order to obtain the joint motion references for a low level controller. As concerns the arm, an impedance filter is adopted in order to make the controller performance independent from the knowledge of the dynamic model, while a pure motion controller is in charge of following motion references. It is worth noting that the impedance filter requires the wrench measured by a force/torque wrist sensor and a compensation term taking into account the effects on the wrist due to hand dynamics and contact forces.

The effectiveness of the proposed control scheme has been experimentally tested on a setup consisting of a 7DOFs Barret WAM with a wrist-mounted 6-axis force/torque sensor, and a BarrettHand, attached on the arm wrist, with joint torques sensors and tactile sensors providing 96 cells of tactile-array data spread across all three fingers and the palm.

II. Modeling

In a robotic arm/hand system the hand (or gripper) is usually mounted on the wrist and, if a wrist force/torque sensor is available, the measurements keep track of the hand dynamics. The only way to compensate these forces, if the wrist has to be reactive only to interaction forces, is by computing a dynamic model of the hand with a floating base (the palm).

978-1-4799-3684-7/14/$31.00 ©2014 IEEE

A. Dynamic model of the floating base hand

Let us define the state of the arm wrist as $\boldsymbol{x}_h = [\ \boldsymbol{p}_h^{\mathrm{T}} \quad \mathcal{Q}_h^{\mathrm{T}}\ ]^{\mathrm{T}}$, where $\boldsymbol{p}_h$ is the vector pointing at the origin of the wrist frame Σ_h, $\mathcal{Q}_h$ is is the unit quaternion $\mathcal{Q}_h = \{\eta_h, \boldsymbol{\epsilon}_h\}$, representing the orientation of Σ_h with respect to the base frame Σ_b. Let us assume that the four components of $\mathcal{Q}_h$ are independent; this assumption will be further removed. In order to determine the dynamics of the floating base hand, a set of lagrangian generalized coordinates is chosen as

$$\boldsymbol{\lambda} = [\ \boldsymbol{x}_h^{\mathrm{T}} \quad \boldsymbol{q}_f^{\mathrm{T}}\ ]^{\mathrm{T}}, \tag{1}$$

where $\boldsymbol{q}_f \in \mathbb{R}^l$ is the vector of finger joint positions, being l the number of joints. The dynamic model can be derived by following the Lagrangian formulation. To this aim the total energy of the system needs to be computed.

1) Kinetic Energy: The kinetic energy of the system can be computed as follows

$$\mathcal{K} = \frac{1}{2}\boldsymbol{v}_h^{\mathrm{T}}\bar{\boldsymbol{M}}_h\boldsymbol{v}_h + \frac{1}{2}\sum_{j=1}^{N}\sum_{i=1}^{f_j}\boldsymbol{v}_i^{j\mathrm{T}}\bar{\boldsymbol{M}}_i^j\boldsymbol{v}_i^j, \tag{2}$$

where $\boldsymbol{v}_h = \left[\dot{\boldsymbol{p}}_h^{\mathrm{T}}\ \boldsymbol{\omega}_h^{\mathrm{T}}\right]^{\mathrm{T}} \in \mathbb{R}^6$ is the twist of the wrist frame Σ_h (which coincides with the arm end-effector frame and the palm frame), $\boldsymbol{\omega}_h$ is the angular velocity of Σ_h, $\bar{\boldsymbol{M}}_h = \mathrm{diag}\{m_h\boldsymbol{I}_3,\ \boldsymbol{M}_h\}$, m_h and $\boldsymbol{M}_h$ are the mass and inertia tensor, respectively, of the wrist, N is the number of finger, f_j is the number of joints of finger j, $\boldsymbol{v}_i^j$ is the generalized velocity (twist) of the frame attached to the Center of Gravity (CoG) of link i belonging to finger j, $\bar{\boldsymbol{M}}_i^j = \mathrm{diag}\{m_i^j\boldsymbol{I}_3,\ \boldsymbol{M}_i^j\}$, m_i^j and $\boldsymbol{M}_i^j$ are the mass and inertia tensor, respectively, of the link i belonging to the jth finger. The twist of the CoG frame of each link, belonging to the jth finger, can be computed as

$$\boldsymbol{v}_i^j \quad = \quad \boldsymbol{G}_{i,h}^{j\mathrm{T}}\boldsymbol{v}_h + \boldsymbol{v}_{i,h}^j, \tag{3}$$

where $i = 1, 2, \ldots, f_j$,

$$\boldsymbol{G}_{i,h}^{j\mathrm{T}}\left(\boldsymbol{p}_{i,h}^j\right) = \begin{bmatrix} \boldsymbol{I}_3 & -\boldsymbol{S}(\boldsymbol{p}_{i,h}^j) \\ \boldsymbol{O}_3 & \boldsymbol{I}_3 \end{bmatrix}, \tag{4}$$

$\boldsymbol{v}_{i,h}^j = \left[\dot{\boldsymbol{p}}_{i,h}^{j\mathrm{T}}\ \boldsymbol{\omega}_{i,h}^{j\mathrm{T}}\right]^T$, $\boldsymbol{p}_{i,h}^j \in \mathbb{R}^3$ is the relative position of the CoG of link i, belonging to finger j, with respect to the palm frame, $\boldsymbol{\omega}_{i,h}^j \in \mathbb{R}^3$ is the relative angular velocity of the CoG of the link i, belonging to finger j, with respect to the palm frame, $\boldsymbol{O}_r$ is the $(r \times r)$ null matrix, $\boldsymbol{I}_r$ is the $(r \times r)$ identity matrix, $\boldsymbol{S}(\cdot) \in \mathbb{R}^{3\times 3}$ is the skew symmetric operator defining the cross product [3]. Linear and angular relative velocities $\dot{\boldsymbol{p}}_{i,h}^j$, $\boldsymbol{\omega}_{i,h}^j$ can be further expressed as

$$\boldsymbol{v}_{i,h}^j = \begin{bmatrix} \dot{\boldsymbol{p}}_{i,h}^j \\ \boldsymbol{\omega}_{i,h}^j \end{bmatrix} = \begin{bmatrix} \boldsymbol{J}_p^{i,j}(\boldsymbol{q}_i^j) \\ \boldsymbol{J}_o^{i,j}(\boldsymbol{q}_i^j) \end{bmatrix}\dot{\boldsymbol{q}}_i^j = \boldsymbol{J}_f^{i,j}\dot{\boldsymbol{q}}_i^j, \tag{5}$$

where $\boldsymbol{q}_i^j = \left[q_1^j, q_2^j, \ldots, q_i^j\right]$, q_i^j is the position of the ith joint belonging to the jth finger, where

$$\boldsymbol{J}_p^{i,j}(\boldsymbol{q}_i^j) = \left[\boldsymbol{J}_{p1}^{i,j}(q_1^j)\ \ \boldsymbol{J}_{p2}^{i,j}(q_2^j)\ \ \ldots\ \ \boldsymbol{J}_{pi}^{i,j}(q_i^j)\ \boldsymbol{0}_{f_j-i}\right],$$

$$\boldsymbol{J}_o^{i,j}(\boldsymbol{q}_i^j) = \left[\boldsymbol{J}_{o1}^{i,j}(q_1^j)\ \ \boldsymbol{J}_{o2}^{i,j}(q_2^j)\ \ \ldots\ \ \boldsymbol{J}_{oi}^{i,j}(q_i^j)\ \boldsymbol{0}_{f_j-i}\right],$$

and $\boldsymbol{J}_{pk}^{i,j}$ ($\boldsymbol{J}_{ok}^{i,j}$) is the Jacobian representing the contribution of joint k to the linear (angular) velocity of the CoG of link i belonging to finger j.

By noting that $\mathcal{W}_h = \{0, \boldsymbol{\omega}_h\} = 2\dot{\mathcal{Q}}_h * \mathcal{Q}_h^{-1}$, the wrist velocity could be written in terms of $\dot{\boldsymbol{x}}_h$

$$\begin{aligned} \boldsymbol{v}_h &= \boldsymbol{L}_h\dot{\boldsymbol{x}}_h, \\ \boldsymbol{L}_h &= \begin{bmatrix} \boldsymbol{I}_3 & \boldsymbol{O}_{3\times 4} \\ \boldsymbol{O}_3 & \bar{\boldsymbol{L}}_h \end{bmatrix}, \bar{\boldsymbol{L}}_h = 2\left[\ \boldsymbol{\epsilon}_h\ \ \eta_h\boldsymbol{I}_3 - \boldsymbol{S}(\boldsymbol{\epsilon}_h)\ \right], \end{aligned} \tag{6}$$

where $\boldsymbol{O}_{r\times s}$ is the $r \times s$ null matrix, and the kinetic energy can be rewritten in the compact form

$$\mathcal{K} = \frac{1}{2}\dot{\boldsymbol{\lambda}}^{\mathrm{T}}\boldsymbol{B}(\boldsymbol{\lambda})\dot{\boldsymbol{\lambda}} = \frac{1}{2}\dot{\boldsymbol{\lambda}}^{\mathrm{T}}\begin{bmatrix} \boldsymbol{B}_{hh}(\boldsymbol{\lambda}) & \boldsymbol{B}_{hf}(\boldsymbol{\lambda}) \\ \boldsymbol{B}_{hf}{}^{\mathrm{T}}(\boldsymbol{\lambda}) & \boldsymbol{B}_{ff}(\boldsymbol{\lambda}) \end{bmatrix}\dot{\boldsymbol{\lambda}}, \tag{7}$$

where $\boldsymbol{B}(\boldsymbol{\lambda})$ is the symmetric and positive definite inertia matrix of the floating base hand, and the block matrices composing $\boldsymbol{B}$ are given by

$$\begin{aligned} \boldsymbol{B}_{hh}(\boldsymbol{\lambda}) &= \boldsymbol{L}_h^{\mathrm{T}}\left(\bar{\boldsymbol{M}}_h + \sum_{j=1}^{N}\sum_{i=1}^{f_j}\boldsymbol{G}_{i,h}^j\bar{\boldsymbol{M}}_i^j\boldsymbol{G}_{i,h}^{j\mathrm{T}}\right)\boldsymbol{L}_h, \\ \boldsymbol{B}_{hf}(\boldsymbol{\lambda}) &= \sum_{j=1}^{N}\sum_{i=1}^{f_j}\boldsymbol{L}_h^{\mathrm{T}}\boldsymbol{G}_{i,h}^j\bar{\boldsymbol{M}}_i^j\boldsymbol{J}_f^{i,j}, \\ \boldsymbol{B}_{ff}(\boldsymbol{\lambda}) &= \sum_{j=1}^{N}\sum_{i=1}^{n_j}\boldsymbol{J}_f^{i,j\mathrm{T}}\bar{\boldsymbol{M}}_i^j\boldsymbol{J}_f^{i,j}. \end{aligned} \tag{8}$$

2) Potential energy: The potential energy of the floating base hand is computed according to

$$\mathcal{T} = m_h\boldsymbol{g}_a^{\mathrm{T}}\boldsymbol{p}_h + \sum_{j=1}^{N}\sum_{i=1}^{f_j}m_i^j\boldsymbol{g}_a^{\mathrm{T}}\boldsymbol{p}_i^j, \tag{9}$$

where $\boldsymbol{g}_a = [0\ 0\ g]^{\mathrm{T}}$ is the gravity acceleration.

It is worth noting that $\boldsymbol{p}_i^j = \boldsymbol{p}_h + \boldsymbol{R}_h\boldsymbol{p}_{i,h}^{jh}$, where $\boldsymbol{p}_{i,h}^{jh}$ is the relative position of the CoG of the link i belonging to finger j with respect to Σ_h, in terms of wrist frame coordinate, as denoted by the superscript h, while

$$\boldsymbol{R}_h(\mathcal{Q}_h) = \eta_h^2\boldsymbol{I}_3 + 2\boldsymbol{\epsilon}_h\boldsymbol{\epsilon}_h^{\mathrm{T}} - 2\eta_h\boldsymbol{S}(\boldsymbol{\epsilon}_h).$$

3) Lagrangian equation: The dynamic model can be stated in the usual form

$$\boldsymbol{B}(\boldsymbol{\lambda})\ddot{\boldsymbol{\lambda}} + \boldsymbol{C}(\boldsymbol{\lambda}, \dot{\boldsymbol{\lambda}})\dot{\boldsymbol{\lambda}} + \boldsymbol{g}(\boldsymbol{\lambda}) = \boldsymbol{\xi}, \tag{10}$$

where $\boldsymbol{C}$ and $\boldsymbol{g}$ are computed according to [3]. The term $\boldsymbol{\xi}$, which represents the generalized forces associated with the generalized coordinates $\boldsymbol{\lambda}$, could be computed by considering the static equilibrium. If the system reaches a static equilibrium, the virtual work is null

$$-\boldsymbol{v}_c^{\mathrm{T}}\boldsymbol{h}_c + \dot{\boldsymbol{q}}_f^{\mathrm{T}}\boldsymbol{\tau}_f - \boldsymbol{v}_h^{\mathrm{T}}\boldsymbol{h}_h = 0, \tag{11}$$

where $\boldsymbol{v}_c \in \mathbb{R}^{6n_c}$ is the vector stacking finger velocities at each contact point, n_c is the number of contact points, $\boldsymbol{h}_c \in \mathbb{R}^{6n_c}$ is the vector stacking the contact wrenches, $\boldsymbol{\tau}_f \in \mathbb{R}^l$ is the vector of commanded torques, $\boldsymbol{h}_h \in \mathbb{R}^6$ represents the wrist wrench. The contact generalized velocities (twists) can be further expressed as

$$\boldsymbol{v}_c = \boldsymbol{G}_h^{\mathrm{T}}(\boldsymbol{r}_h)\boldsymbol{v}_h + \boldsymbol{J}_{f_c}\dot{\boldsymbol{q}}_f\,, \tag{12}$$

where $\boldsymbol{r}_h$ is the vector stacking the position of each contact point with respect to the wrist frame,

$$\boldsymbol{G}_h(\boldsymbol{r}_h) = \begin{bmatrix} \boldsymbol{G}_{h_1}(\boldsymbol{r}_{h_1}) & \boldsymbol{G}_{h_2}(\boldsymbol{r}_{h_2}) & \dots & \boldsymbol{G}_{h_{n_c}}(\boldsymbol{r}_{h_{n_c}}) \end{bmatrix},$$

$$\boldsymbol{G}_{h_i}(\boldsymbol{r}_{h_i}) = \begin{bmatrix} \boldsymbol{I}_3 & \boldsymbol{O}_3 \\ \boldsymbol{S}(\boldsymbol{r}_{h_i}) & \boldsymbol{I}_3 \end{bmatrix},$$

$\boldsymbol{J}_{f_c}$ is the hand Jacobian mapping the joint velocities into contact point twists. The principle of virtual works becomes

$$-\dot{\boldsymbol{x}}_h^{\mathrm{T}}\boldsymbol{L}_h^{\mathrm{T}}\left(\boldsymbol{h}_h + \boldsymbol{G}_h(\boldsymbol{r}_h)\boldsymbol{h}_c\right) + \dot{\boldsymbol{q}}_f^{\mathrm{T}}\left(\boldsymbol{\tau}_f - \boldsymbol{J}_{f_c}^{\mathrm{T}}\boldsymbol{h}_c\right) = 0, \tag{13}$$

from which it could be recognized that

$$\boldsymbol{\xi} = \begin{bmatrix} -\boldsymbol{L}_h^{\mathrm{T}}\left(\boldsymbol{h}_h + \boldsymbol{G}_h(\boldsymbol{r}_h)\boldsymbol{h}_c\right) \\ \boldsymbol{\tau}_f - \boldsymbol{J}_{f_c}^{\mathrm{T}}\boldsymbol{h}_c \end{bmatrix}. \tag{14}$$

Since a non-minimal representation has been chosen for the orientation of the wrist frame, the so-called lagrangian variables, i.e. the component of the vector $\boldsymbol{\lambda}$, are not independent: 4 of them are constrained via the following relation

$$\phi(\boldsymbol{\lambda}) = \frac{1}{2}\left(1 - \boldsymbol{\lambda}^{\mathrm{T}}\boldsymbol{Q}^{\mathrm{T}}\boldsymbol{Q}\boldsymbol{\lambda}\right) = 0, \tag{15}$$

where $\boldsymbol{Q} = [\boldsymbol{O}_3\ \boldsymbol{I}_4\ \boldsymbol{O}_l]$ and l is the number of the hand's joint. The constraint expressed via (15) establishes that $\mathcal{Q}_h$ must be a unit quaternion. Finally, according to [1], the lagrangian equation should include the constraint (15)

$$\boldsymbol{B}(\boldsymbol{\lambda})\ddot{\boldsymbol{\lambda}} + \boldsymbol{C}(\boldsymbol{\lambda},\dot{\boldsymbol{\lambda}})\dot{\boldsymbol{\lambda}} + \boldsymbol{g}(\boldsymbol{\lambda}) + \beta\left(\frac{\partial\phi}{\partial\boldsymbol{\lambda}}\right)^{\mathrm{T}} = \boldsymbol{\xi}. \tag{16}$$

By noting that $\partial\phi/\partial\boldsymbol{\lambda} = -\boldsymbol{Q}^{\mathrm{T}}\boldsymbol{Q}\boldsymbol{\lambda}$, equation (16) can be rewritten as

$$\boldsymbol{B}(\boldsymbol{\lambda})\ddot{\boldsymbol{\lambda}} + \boldsymbol{C}(\boldsymbol{\lambda},\dot{\boldsymbol{\lambda}})\dot{\boldsymbol{\lambda}} + \boldsymbol{g}(\boldsymbol{\lambda}) = \boldsymbol{\xi} + \beta\boldsymbol{Q}^{\mathrm{T}}\boldsymbol{Q}\boldsymbol{\lambda}, \tag{17}$$

from which β can be computed by pre-multiplying the (17) by $\boldsymbol{\lambda}^{\mathrm{T}}$, obtaining

$$\beta = \boldsymbol{\lambda}^{\mathrm{T}}\left(\boldsymbol{B}(\boldsymbol{\lambda})\ddot{\boldsymbol{\lambda}} + \boldsymbol{C}(\boldsymbol{\lambda},\dot{\boldsymbol{\lambda}})\dot{\boldsymbol{\lambda}} + \boldsymbol{g}(\boldsymbol{\lambda}) - \boldsymbol{\xi}\right). \tag{18}$$

By folding (18) into (17) and after few algebraic steps, it yields

$$\boldsymbol{B}(\boldsymbol{\lambda})\ddot{\boldsymbol{\lambda}} + \bar{\boldsymbol{C}}(\boldsymbol{\lambda},\dot{\boldsymbol{\lambda}})\dot{\boldsymbol{\lambda}} + \bar{\boldsymbol{g}}(\boldsymbol{\lambda}) = \bar{\boldsymbol{\xi}} - \boldsymbol{B}(\boldsymbol{\lambda})\boldsymbol{\lambda}\dot{\boldsymbol{\lambda}}^{\mathrm{T}}\boldsymbol{Q}^{\mathrm{T}}\boldsymbol{Q}\dot{\boldsymbol{\lambda}}, \tag{19}$$

where $\bar{(*)} = \left(\boldsymbol{I}_{7+f} - \boldsymbol{Q}^{\mathrm{T}}\boldsymbol{Q}\boldsymbol{\lambda}\boldsymbol{\lambda}^{\mathrm{T}}\right)(*)$ and $(*) = \{\boldsymbol{C}, \boldsymbol{g}, \boldsymbol{\xi}\}$.

B. Object dynamics

The contact model is assumed to be point contact with friction (hard finger) and, thus, the contact wrenches, at the jth contact, can be written as $\boldsymbol{h}_{c_j} = [\boldsymbol{f}_{c_j}^{\mathrm{T}}\ \boldsymbol{0}_3^{\mathrm{T}}]^{\mathrm{T}}$, where $\boldsymbol{f}_{c_j} \in \mathbb{R}^3$ is the force exerted by the finger on the object. In the general case, the object could interact also with the external environment (obstacles, or other objects) and the dynamic model must include the environmental interaction wrench, $\boldsymbol{h}_e \in \mathbb{R}^6$. The detailed dynamics of the grasped object can be expressed via the following

$$\boldsymbol{B}_o\dot{\boldsymbol{v}}_o + \boldsymbol{C}(\boldsymbol{v}_o)\boldsymbol{v}_o + \boldsymbol{g}_o = \boldsymbol{G}(\boldsymbol{r}_o)\boldsymbol{f}_c - \boldsymbol{h}_e, \tag{20}$$

where $\boldsymbol{B}_o = \mathrm{diag}\{m_o\boldsymbol{I}_3, \boldsymbol{M}_o\}$, $m_o \in \mathbb{R}$ and $\boldsymbol{M}_o \in \mathbb{R}^{3\times3}$ are the mass and inertia tensor of the object, $\boldsymbol{v}_o \in \mathbb{R}^6$ is the generalized velocity of a frame attached to the center of gravity (CoG) of the object, $\boldsymbol{C}(\boldsymbol{v}_o) \in \mathbb{R}^{6\times6}$ is the matrix collecting the centrifugal and Coriolis terms, $\boldsymbol{g}_o \in \mathbb{R}^6$ is the gravity generalized force, $\boldsymbol{f}_c \in \mathbb{R}^{3n_c}$ is the vector stacking the contact forces, $\boldsymbol{G}(\boldsymbol{r}_o) \in \mathbb{R}^{6\times3n_c}$ is the grasp matrix

$$\boldsymbol{G}(\boldsymbol{r}_o) = \begin{bmatrix} \boldsymbol{G}_1(\boldsymbol{r}_{o_1}) & \boldsymbol{G}_2(\boldsymbol{r}_{o_2}) & \dots & \boldsymbol{G}_{n_c}(\boldsymbol{r}_{o_{n_c}}) \end{bmatrix}, \tag{21}$$

$\boldsymbol{G}_i(\boldsymbol{r}_{o_i}) = \begin{bmatrix} \boldsymbol{I}_3^{\mathrm{T}}\ \boldsymbol{S}(\boldsymbol{r}_{o_i})^{\mathrm{T}} \end{bmatrix}^{\mathrm{T}}$, $\boldsymbol{r}_o = \begin{bmatrix}\boldsymbol{r}_{o_1}^{\mathrm{T}}\ \boldsymbol{r}_{o_2}^{\mathrm{T}}, \dots\ \boldsymbol{r}_{o_{n_c}}^{\mathrm{T}}\end{bmatrix}^{\mathrm{T}}$ and $\boldsymbol{r}_{o_i} \in \mathbb{R}^3$ is the relative position of the ith contact point with respect to the object reference point. If $\mathrm{rank}(\boldsymbol{G}(\boldsymbol{r}_o)) = 6$ and $n_c > 2$ there exists a set of forces $\boldsymbol{f}_{c_I} \in \mathbb{R}^{3n_c}$, the so-called internal contact forces, such that $\boldsymbol{G}(\boldsymbol{r}_o)\boldsymbol{f}_{c_I} = \boldsymbol{0}_6$. In other words, $\boldsymbol{f}_{c_I}$ represent forces not affecting the object motion; thus, they represent internal stresses applied to the object. On the other hand, contact forces which affect object dynamics, are called external contact forces $\boldsymbol{f}_{c_E} \in \mathbb{R}^{3n_c}$. The forces exerted by fingertips on the object are the sum of the internal contact forces and the external ones $\boldsymbol{f}_c = \boldsymbol{f}_{c_E} + \boldsymbol{f}_{c_I}$.

III. Control Architecture

Grasping and manipulation of an object require fine control of internal contact forces, in order to stabilize the grasp when the object is moved along a planned trajectory. Internal force control should prevent contact breaks and/or excessive stresses on the object.

The control system should be able to deal with all those events involving environmental or human interaction in safety conditions. A way to guarantee a safe behavior of the manipulation system is that of resorting to an impedance control scheme, which ensure good tracking of the reference trajectory in absence of interaction, while enforcing a compliant behavior when an unexpected interaction happens.

A. Hand control

Robotic hands are not usually torque controlled since the actuation system could be very complex, due to space limitation and, thus, it would be useful to compute motion references of the fingers through a dynamic planner. A low level controller, often embedded, is in charge of tracking joint references. Let Σ_{c_j} be a reference frame, hereafter contact frame, attached to the object at the jth contact point. By assuming that only fingertips are involved in grasping (fine manipulation), i.e. the number of contact points and fingers is the same, the dynamic planner for finger j, designed to control internal forces, is given by

$$\begin{aligned} &\boldsymbol{M}_{d_f}\dot{\boldsymbol{\nu}}_{d_j}^{c_j} + \boldsymbol{K}_{d_f}\boldsymbol{\nu}_{d_j}^{c_j} + \boldsymbol{K}_{p_f}\widetilde{\boldsymbol{x}}_{d_j}^{c_j} = \boldsymbol{K}_{p_f}\boldsymbol{x}_{f_j}^{c_j} \\ &\boldsymbol{x}_{f_j}^{c_j} = \boldsymbol{C}_f(\boldsymbol{h}_{I_{d_j}}^{c_j} - \boldsymbol{h}_{I_j}^{c_j}) + \boldsymbol{C}_I\int_0^t(\boldsymbol{h}_{I_{d_j}}^{c_j} - \boldsymbol{h}_{I_j}^{c_j})\mathrm{d}\sigma, \end{aligned} \tag{22}$$

where the superscript c_j means that vectors are expressed in terms of coordinates of Σ_{c_j}, $\dot{\boldsymbol{\nu}}_{d_j}^{c_j} \in \mathbb{R}^{6\times1}$ ($\boldsymbol{\nu}_{d_j}^{c_j} \in \mathbb{R}^{6\times1}$)

is the relative reference accelerations (velocities) of contact points with respect to Σ_h, $\widetilde{\boldsymbol{x}}_{d_j} = \left[\widetilde{\boldsymbol{r}}_{d_j}{}^{\mathrm{T}}\, \widetilde{\boldsymbol{\epsilon}}_{d_j}{}^{\mathrm{T}}\right]^{\mathrm{T}}$, $\widetilde{\boldsymbol{r}}_{d_j} = \boldsymbol{r}_{d_j} - \boldsymbol{r}_{s_j}$, where $\boldsymbol{r}_{s_j}$, $\boldsymbol{r}_{d_j}$ have the meaning of rest and reference positions relative to Σ_h, $\widetilde{\boldsymbol{\epsilon}}_{d_j}$ is the vector part of the quaternion extracted from $\widetilde{\mathcal{Q}}_j = \mathcal{Q}_{h,s_j} * \mathcal{Q}_{h,d_j}^{-1}$ the orientation error of finger j, where $\mathcal{Q}_{h,s_j}$, $\mathcal{Q}_{h,d_j}$ represent the rest and the reference orientation, of the contact frame with respect to Σ_h, $\boldsymbol{M}_{d_f}$, $\boldsymbol{K}_{d_f}$, $\boldsymbol{K}_{p_f}$, $\boldsymbol{C}_f$, $\boldsymbol{C}_I$, are positive definite matrices of gains, $\boldsymbol{h}_{I_{d_j}} = [\boldsymbol{f}_{I_{d_j}}^{\mathrm{T}}\ \boldsymbol{0}_3^{\mathrm{T}}]^{\mathrm{T}}$ is vector of desired internal wrenches, $\boldsymbol{h}_{I_j} = [\boldsymbol{f}_{I_j}^{\mathrm{T}}\ \boldsymbol{0}_3^{\mathrm{T}}]^{\mathrm{T}}$ is the vector of measured internal generalized forces. Desired internal forces can be achieved via standard grasp force optimization techniques [17], to avoid slippage and excessive mechanical stresses on the object.

By integrating equation (22), motion references in Cartesian space are available to feed an Inverse Kinematics (IK) algorithm.

B. Arm control

The aim is that of making the wrist able to track the desired trajectory with good accuracy in the absence of any interaction, while a compliant behavior is expected if interactions occur: this could be achieved via an impedance control law. More in detail, an impedance filter is adopted in order to make the controller performance independent from the knowledge of the dynamic model, while a pure motion controller is in charge of following the motion references. The desired impedance has the following dynamics

$$\boldsymbol{M}_d \dot{\widetilde{\boldsymbol{v}}}_h + \boldsymbol{K}_d \widetilde{\boldsymbol{v}}_h + \boldsymbol{h}_{\Delta p} = \boldsymbol{h}_h - \boldsymbol{h}_{comp}, \tag{23}$$

where, $\boldsymbol{M}_d$, $\boldsymbol{K}_d$ are positive definite matrices, $\dot{\widetilde{\boldsymbol{v}}}_h$ ($\widetilde{\boldsymbol{v}}_h$) is the acceleration (velocity) error, computed as the difference between the desired acceleration (velocity) $\dot{\boldsymbol{v}}_{h_d}$ ($\boldsymbol{v}_{h_d}$) planned off-line and the reference one $\dot{\boldsymbol{v}}_{h_r}$ ($\boldsymbol{v}_{h_r}$),

$$\boldsymbol{h}_{\Delta p} = \begin{bmatrix} \boldsymbol{K}_p & \boldsymbol{O}_3 \\ \boldsymbol{O}_3 & \boldsymbol{K}_o \end{bmatrix} \begin{bmatrix} \widetilde{\boldsymbol{p}}_{dr} \\ \widetilde{\varepsilon}_{dr} \end{bmatrix}, \tag{24}$$

where $\boldsymbol{K}_p$ and $\boldsymbol{K}_o$ are positive definite matrices of gains, $\widetilde{\boldsymbol{p}}_{dr}$ is the position error, $\widetilde{\mathcal{Q}}_{dr} = \left[\widetilde{\eta}_{dr}\ \ \widetilde{\boldsymbol{\epsilon}}_{dr}^{\mathrm{T}}\right]^{\mathrm{T}}$ is the quaternion representing the relative orientation between the desired and reference orientation of the frame Σ_h. The other terms in (23) are $\boldsymbol{h}_h$, which is the wrench measured by the sensor, and $\boldsymbol{h}_{comp}$, which is a compensation of the effects on the wrist due to hand dynamics and contact forces, computed through the first 7 equations of (16) as

$$\boldsymbol{h}_{comp} = -\left(\boldsymbol{G}_h^{\mathrm{T}}(\boldsymbol{r}_h)\boldsymbol{h}_c + (\boldsymbol{L}_h\boldsymbol{L}_h^{\mathrm{T}})^{-1}\boldsymbol{L}_h\boldsymbol{H}_7\boldsymbol{\xi}\right),$$

where $\boldsymbol{H}_\alpha$ is a selector operator extracting the first α components from a (larger) vector of dimension n, namely $\boldsymbol{H}_\alpha = \left[\ \boldsymbol{I}_\alpha \quad \boldsymbol{O}_{\alpha,n-\alpha}\ \right]$. Once the motion references are known, a motion controller, directly designed in the operational space, could be fed. An alternative way is that of performing an IK algorithm to compute joint reference trajectories in such a way to feed a more reliable joint level controller.

Remark 1: If the dynamic parameters of the hand are not available it could be enough to compensate the static effects of the hand and the contact forces,

$$\boldsymbol{h}_{comp} = -\left(\boldsymbol{G}_h(\boldsymbol{r}_h)\boldsymbol{h}_c + (\boldsymbol{L}_h\boldsymbol{L}_h^{\mathrm{T}})^{-1}\boldsymbol{L}_h\boldsymbol{H}_7\boldsymbol{g}(\boldsymbol{\lambda})\right). \tag{25}$$

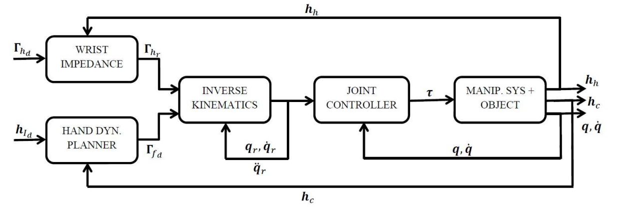

Fig. 1. Block scheme of the control architecture. Γ_{h_d} represents the desired trajectory, in terms of pose, velocities and accelerations, for the wrist while Γ_{h_r} (Γ_{f_d}) represent the reference trajectory for the wrist (contact points)

C. Joint references

Since (22) and (23) provide motion references in Cartesian space, an IK algorithm is needed to compute suitable joint references in order to feed a low level controller, as shown in Fig. 1. A possible choice is given by the following law

$$\ddot{\boldsymbol{q}}_r = \boldsymbol{J}^{-1}\left(\dot{\boldsymbol{v}}_r + \boldsymbol{K}_v\boldsymbol{e}_v + \boldsymbol{K}\boldsymbol{e}_p - \dot{\boldsymbol{J}}\dot{\boldsymbol{q}}_r\right), \tag{26}$$

where $\boldsymbol{q}_r = [\boldsymbol{q}_{h_r}^{\mathrm{T}}\ \boldsymbol{q}_{f_r}^{\mathrm{T}}]^{\mathrm{T}}$ is the vector stacking joint arm $\boldsymbol{q}_{h_r}$ and hand $\boldsymbol{q}_{f_h}$ positions, $\boldsymbol{J}$ is the following Jacobian

$$\boldsymbol{J} = \begin{bmatrix} \boldsymbol{J}_h & \boldsymbol{O}_{6n\times l} \\ \boldsymbol{O}_{6n_c\times n_h} & \boldsymbol{J}_f \end{bmatrix},$$

n_h is the number of arm DOFs, $l = \sum_{i=1}^{N} f_j$ is the number of hand DOFs, $\boldsymbol{v}_r = \left[\boldsymbol{v}_{h_r}^{\mathrm{T}}\ \boldsymbol{\nu}_d^{\mathrm{T}}\right]^{\mathrm{T}}$, $\boldsymbol{\nu}_d \in \mathbb{R}^{6n_c\times 1}$ is the vector staking all relative reference finger twists, $\boldsymbol{e}_v$ is the velocity error, i.e. $\boldsymbol{e}_v = \boldsymbol{v}_r - \boldsymbol{J}\dot{\boldsymbol{q}}_r$, $\boldsymbol{e}_p = \left[\widetilde{\boldsymbol{p}}_h^{\mathrm{T}}\ \widetilde{\boldsymbol{\epsilon}}_h^{\mathrm{T}}\ \widetilde{\boldsymbol{r}}_{re}^{\mathrm{T}}\ \widetilde{\boldsymbol{\epsilon}}_{re}^{\mathrm{T}}\right]^{\mathrm{T}}$, $\widetilde{\boldsymbol{p}}_h$ ($\widetilde{\boldsymbol{r}}_{re}$) is the position error of the wrist (finger), i.e. the difference between the reference value and that computed via the forward kinematics on the basis of $\boldsymbol{q}_{h_r}$ ($\boldsymbol{q}_{f_r}$), $\widetilde{\boldsymbol{\epsilon}}_h$ is the vector part of the unit quaternion $\widetilde{\mathcal{Q}}_h = \mathcal{Q}_{r_h} * \mathcal{Q}_{e_h}^{-1}$, where $\mathcal{Q}_{r_h}$ and $\mathcal{Q}_{e_h}$ represent the reference orientation and that computed via the forward kinematics on the basis of $\boldsymbol{q}_{h_r}$, $\widetilde{\varepsilon}_{re} = \left[\widetilde{\boldsymbol{\epsilon}}_{r_1}^{\mathrm{T}}\ \widetilde{\boldsymbol{\epsilon}}_{r_2}^{\mathrm{T}} \ldots, \widetilde{\boldsymbol{\epsilon}}_{r_{n_c}}^{\mathrm{T}}\right]^{\mathrm{T}}$ and $\widetilde{\boldsymbol{\epsilon}}_{r_j}$ is the vector part of the quaternion $\widetilde{\mathcal{Q}}_{rj} = \mathcal{Q}_{r_j} * \mathcal{Q}_{e_j}^{-1}$ representing the orientation error of finger j, where $\mathcal{Q}_{r_j}$ and $\mathcal{Q}_{e_j}$ are the reference and that computed via the direct kinematics on the basis of $\boldsymbol{q}_{f_r}$.

Remark 2: If the arm/hand system is redundant, i.e. $\boldsymbol{J}$ has more columns than rows, (26) should be suitably modified

$$\ddot{\boldsymbol{q}}_r = \boldsymbol{J}^{\dagger}(\dot{\boldsymbol{v}}_r + \boldsymbol{K}_v\boldsymbol{e}_v + \boldsymbol{K}\boldsymbol{e}_p - \dot{\boldsymbol{J}}\dot{\boldsymbol{q}}_r) - \boldsymbol{N}_J(\dot{\boldsymbol{N}}_J + k_s)\dot{\boldsymbol{q}}, \tag{27}$$

where $\boldsymbol{J}^{\dagger}$ is a right pseudo-inverse of $\boldsymbol{J}$, $\boldsymbol{N}_J$ is a null space projector and $-(\dot{\boldsymbol{N}}_J + k_s)\dot{\boldsymbol{q}}$ is a term designed to stabilize internal motions. A stability proof of (27) is reported in Appendix A.

IV. CASE STUDY

Experiments have been conducted in order to test the performance of the proposed scheme. The experimental setup, available at the Computer Science Robotics Laboratory of the Rensselaer Polytechnic Institute (RPI), Troy, New York, consists of a 7-DOFs Barret WAM and a Barrett Hand 280

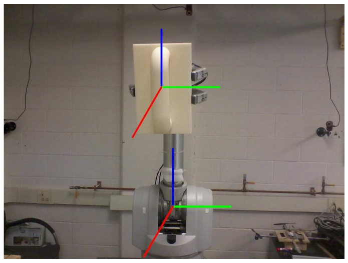

Fig. 2. Experimental setup in the initial configuration. The reference frames are visible: base frame on the bottom and object frame on the top. The axes are ordered as follows: x red, y green, z blue

attached to the arm wrist. The available feedback consists of joint positions, sampled at 500 Hz for the arm and 100 Hz for the hand, force/torque at the wrist, sampled at 500 Hz and tactile pressure on the fingertip and palm (4 matrices of 24 sensors each), sampled at 40 Hz. Robot Operating System (ROS) [18] is used to control the whole system.

Tactile pressures are integrated on the fingertip surfaces in order to estimate the normal contact forces. Since the hand is underactuated and only normal contact forces are available as feedback, the control law (22) has been projected along the normal to the object surface at each contact point, hereafter contact normal. The hand has 4 motors, one for each finger and the forth for the spread, which is the motion of fingers 1 and 2 around the axis normal to the palm. The spread has been kept constant and set to zero. By neglecting the spread contribution, the positional part of the hand Jacobian, $\boldsymbol{J}_f^p \in \mathbb{R}^{9\times 3}$, can be written as $\boldsymbol{J}_f^p = \mathrm{diag}\left\{\boldsymbol{J}_{f_1}^p, \boldsymbol{J}_{f_2}^p, \boldsymbol{J}_{f_3}^p\right\}$, where $\boldsymbol{J}_{f_j}^p \in \mathbb{R}^3$ is the jth finger Jacobian. Because of the underactuation, each $\boldsymbol{J}_{f_j}^p$ has been projected along the contact normal, therefore the Jacobian used in (26) is

$$\boldsymbol{J} = \begin{bmatrix} \boldsymbol{J}_h & \boldsymbol{O}_{6\times 3} \\ \boldsymbol{O}_{3\times n_h} & \boldsymbol{J}_f^n \end{bmatrix},$$

where $\boldsymbol{J}_f^n = \mathrm{diag}\{J_{f_1}^n, J_{f_2}^n, J_{f_3}^n\}$, $J_{f_j}^n = \boldsymbol{n}_j^{\mathrm{T}} \boldsymbol{J}_{f_j}^p$ and $\boldsymbol{n}_j$ is the jth contact normal.

The performed case study consists of a first phase in which the object is grasped by the hand and the contact forces are regulated at suitable values; once the grasp is made, the object is moved along a planned trajectory while a human operator interacts with the object itself: the idea is that of ensuring a compliant behavior maintaining, at the same time, a firm grasp. At the end of the trajectory the object is pressed against a planar surface without neither sliding on it or human operator interaction.

A. Experimental results

The hand grasps the object in such a configuration that the fingertips are symmetric with respect to the object CoG, as depicted in Fig. 2: contact normal forces are regulated to 5 N for finger 1 and 2, and 10 N for the thumb. It can be recognized that the desired normal forces are a set of internal forces since they constitute a self-balancing system. Despite the low rate at which the tactile pressures data are sampled, 40 Hz, the controller, which runs at 100 Hz, is able to drive the contact forces to the desired values, within an acceptable

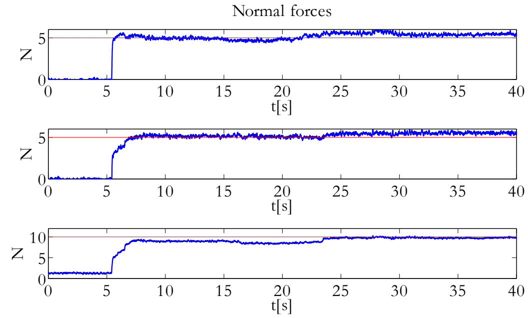

Fig. 3. Time history of the normal contact forces: finger 1 on the top, finger 2 on the middle and thumb on the bottom

error as shown in Fig. 3. For the first 24 s the object is grabbed and the normal contact forces are regulated, in the last 16 s the trajectory is executed. After the object has been grasped, starting from the initial configuration, depicted in Fig. 4(a), the object should be moved of -0.5 m along the z axis and 0.3 m along the x axis of the base frame, while maintaining the position along the y axis. The trajectory has been generated using fifth order polynomial time profile. The final orientation should be such that the x axis of the object frame will be parallel to the x axis of the world frame.

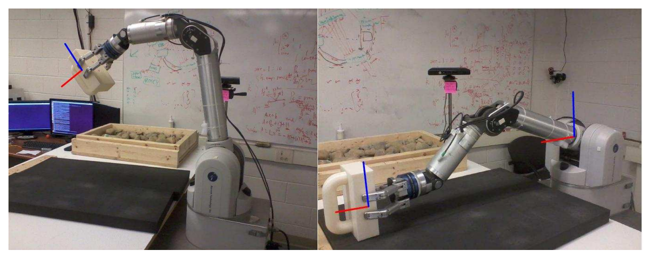

(a) Initial configuration (b) Final configuration

Fig. 4. Initial configuration (a) and final configuration (b) of the system

During the motion, a human operator interacts with the object, by pushing or pulling the handle attached on it, as shown in Fig. 5. It is worth noting that only static compensation has been performed according to (25). The manipulation system should not be compliant along and around the y axis of the base frame, i.e., the measured component of wrist forces and moment are not fed to the impedance filter. The IK errors of the object, both in terms of position and orientation, are shown in Fig. 6: good tracking of the motion reference is ensured, at planning level.

Fig. 7 shows the pose error of the object: it could be recognized that along the y direction there is a good tracking of the planned position while a certain error is observed along the compliant directions. Around 32 s the object interacts with a planar horizontal surface: this explains the large error at steady state. The same consideration can be done for the orientation error: the presence of the steady state error can be justified considering that the surface is not either perfectly horizontal or planar.

V. Conclusions

An experimental study of an arm/hand system has been presented exploiting the impedance paradigm and internal

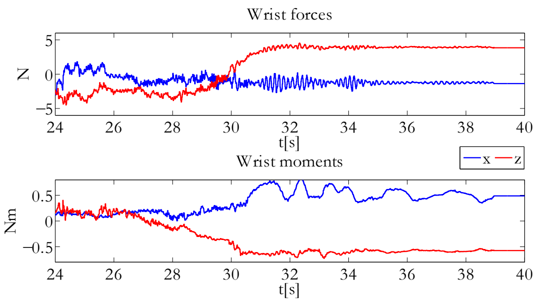

Fig. 5. Time history of the interaction wrist forces and torques

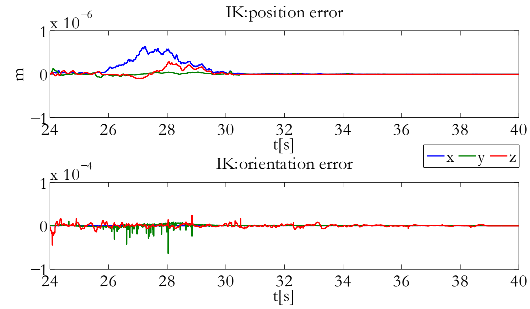

Fig. 6. Time history of closed loop inverse kinematics error

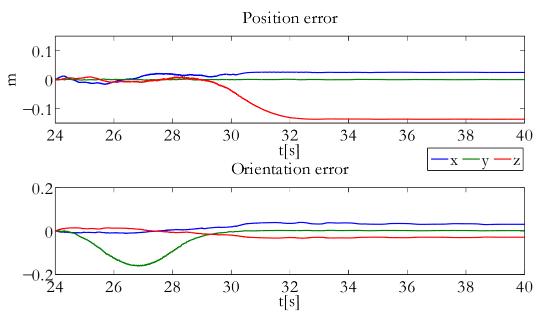

Fig. 7. Time history of the object pose error

force control in order to ensure a compliant behavior and a firm grasp of an object. The interaction has been done by a human operator pushing/pulling the object around and by hitting a planar surface at the end of the trajectory: experimental results show that object is held in any case.

Appendix A

The law (27) could be analyzed in two different orthogonal domains, in the Cartesian space and in the null space of $\boldsymbol{J}$. In Cartesian space, the asymptotic convergence of $\boldsymbol{e}_p$, $\boldsymbol{e}_v$ has been already proven [3]. In internal motion joint space, according to [19], consider the Lyapunov candidate function

$$V_o = \frac{1}{2}\dot{\boldsymbol{q}}_0^{\mathrm{T}}\dot{\boldsymbol{q}}_0, \tag{28}$$

where $\dot{\boldsymbol{q}}_0$ is the vector of joint velocities in the null space of $\boldsymbol{J}$, which can be computed as $\dot{\boldsymbol{q}}_0 = \boldsymbol{N}_J\dot{\boldsymbol{q}}$; by taking the time derivative of $\dot{\boldsymbol{q}}_o$ it yields $\ddot{\boldsymbol{q}}_0 = \dot{\boldsymbol{N}}_J\dot{\boldsymbol{q}} + \boldsymbol{N}_J\ddot{\boldsymbol{q}}$. The time derivative of V_0 is given by

$$\dot{V}_0 = \dot{\boldsymbol{q}}_0^{\mathrm{T}}\ddot{\boldsymbol{q}}_0 = \dot{\boldsymbol{q}}_0^{\mathrm{T}}\boldsymbol{N}_J\ddot{\boldsymbol{q}} + \dot{\boldsymbol{q}}_0^{\mathrm{T}}\boldsymbol{N}_J\dot{\boldsymbol{N}}_J\dot{\boldsymbol{q}}, \tag{29}$$

by recalling (27), by noting that $\boldsymbol{N}_J = \boldsymbol{N}_J^{\mathrm{T}}$ and $\boldsymbol{N}_J\boldsymbol{J}^{\dagger} = \boldsymbol{O}$, after some computation, the (29) becomes

$$\dot{V}_0 = -k_s||\dot{\boldsymbol{q}}_0||^2,\ k_s > 0, \tag{30}$$

which is negative definite. Since $V_0 = \frac{1}{2}||\dot{\boldsymbol{q}}_0||^2$ and $\dot{V}_0 = -k_s||\dot{\boldsymbol{q}}_0||^2$, the equilibrium $\dot{\boldsymbol{q}}_0 = \boldsymbol{0}$ is exponentially stable, moreover, being V_0 radially unbounded, the result holds globally.

Acknowledgment

The research activity of Giuseppe Muscio is supported by ASI (Agenzia Spaziale Italiana). The work of Jeff Trinkle was partially supported by the National Science Foundation (CCF-1208468).

References

[1] R.M. Murray, Z.X. Li, S.S. Sastry, *A mathematical introduction to robotic manipulation*, CRC press, Boca Raton, 1993.

[2] D. Prattichizzo, J.C. Trinkle, "Grasping", *Handbook of Robotics, B. Siciliano and O. Khatib, Eds. Berlin: Springer*, pp. 671–700, 2008.

[3] B. Siciliano, L. Sciavicco, L. Villani, G. Oriolo, "Robotics. Modelling, Planning and Control", *Springer*, 2009.

[4] Robert G. Bonitz, T.C. Hsia, "Internal force-based impedance control for cooperating manipulators," *IEEE Transaction on Robotics and Automation*, vol. 12, no. 1, pp. 78–89, 1996.

[5] F. Caccavale, P. Chiacchio, A. Marino, L.Villani, "Six-DOF Impedance Control of Dual Arm Cooperative Manipulators", *IEEE Transactions On Mechatronics* , vol. 13, pp. 576–587, 2008.

[6] S. Stramigioli, C. Melchiorri, S. Andreotti, "A passivity based control scheme for robotic grasping and manipulation", *Proc. of the 38th Conf. on Decision and Control*, pp. 2951–2956, 1999.

[7] T. Wimboeck, C. Ott, G. Hirzinger, "Analysis and experimental evaluation of the intrinsically passive controller (IPC) for multi-fingered hands", *Proc. of 2008 IEEE Int. Conf. on Robotics and Automation*, pp. 278–284, 2008.

[8] T. Schlegl, M. Buss, T. Omata, G. Schmidt, "Fast dexterous regrasping with optimal contract forces and contact sensor-based impedance control", *Proc. of 2001 IEEE Int. Conf. on Robotics and Automation*, pp. 103–108, 2001.

[9] Z. Chen, N. Lii, M. Jin, S. Fan, H. Liu, "Cartesian Impedance Control on Five-Finger Dexterous Robot Hand DLR-HIT II with Flexible Joint" in *Intelligent Robotics and Applications*, H. Liu, H. Ding, Z. Xiong, X. Zhu Eds. Springer Berlin Heidelberg, 2010.

[10] M.E Abdallah, C.W. Wampler, R. Platt, "Object impedance control using a closed-chain task definition" *2010 10th IEEE-RAS Int. Conf. on Humanoid Robots (Humanoids)*, pp. 269 – 274,2010

[11] K. Nagai, T. Yoshikawa, "Dynamic manipulation/grasping control of multi-fingered robot hands", *Proc. of 1993 IEEE Int. Conf. on Robotics and Automation*, pp. 1027–1033, 1993.

[12] K. Terashima, T. Miyoshi, K. Mouri, H. Kitagawa, P. Minyong, "Hybrid Impedance Control of Massage Considering Dynamic Interaction of Human and Robot Collaboration Systems" *Journal of Robotics and Mechatronics*, Vol.21, No.1 pp. 146-155, 2009.

[13] S. Chiaverini, L. Sciavicco, "The parallel approach to force/position control of robotic manipulators", *IEEE Transactions on Robotics and Automation*, vol. 4, pp. 361–373, 1993.

[14] Y. Karayiannidis, Z. Doulgeri, "Force/Position Regulation for a Robotic Finger in Compliant Contact with an Unknown Surface," *Proc. of the 2005 IEEE Int. Symposium on Intelligent Control, 2005, Mediterrean Conf. on Control and Automation*, pp.77–82, 2005.

[15] F. Caccavale, V. Lippiello, G. Muscio, F. Pierri, F. Ruggiero, L. Villani, "Kinematic control with force feedback for a redundant bimanual manipulation system", *Proc. of 2011 IEEE/RSJ Int. Conf. on Intelligent Robots and Systems*, pp. 4194–4200, 2011.

[16] F. Caccavale, V. Lippiello, G. Muscio, F. Pierri, F. Ruggiero, L. Villani, "Grasp planning and parallel control of a redundant dual-arm/hand manipulation system, , *Robotica*, vol. 31 (7), pp. 1169-1194, 2013.

[17] Y. Nakamura, K. Nagai, T. Yoshikawa, "Dynamics and stability in coordination of multiple robotic mechanisms", *The Int. Journal of Robotics Research* , vol. 8, pp. 44–61, 1989.

[18] M. Quigley, K. Conley, B. P. Gerkey, J. Faust, T. Foote, J. Leibs, R. Wheeler, A.Y. Ng, "ROS: an open-source Robot Operating System", *ICRA Workshop on Open Source Software,* 2009.

[19] P. Hsu, J. Hauser, S. Sastry, "Dynamic Control of Redundant Manipulators", *IEEE Int. Conf. on Robotics and Automation*, vol. 1, pp. 183-187, 1988.